A R C H I V E S O F M E T A L L U R G Y A N D M A T E R I A L S
Volume 60 2015 Issue 3
DOI: 10.1515/amm-2015-0275

P. BULIŃSKI*,#, J. SMOŁKA*, S. GOLAK**, R. PRZYŁUCKI**, L. BLACHA***, R. BIAŁECKI*, M. PALACZ*, G. SIWIEC***

EFFECT OF TURBULENCE MODELLING IN NUMERICAL ANALYSIS OF MELTING PROCESS IN AN INDUCTION FURNACE

WPŁYW MODELU TURBULENCJI NA WYNIKI ANALIZY NUMERYCZNEJ PROCESU TOPIENIA W PIECU INDUKCYJNYM

In this paper, the velocity field and turbulence effects that occur inside a crucible of a typical induction furnace were investigated. In the first part of this work, a free surface shape of the liquid metal was measured in a ceramic crucible. Then a numerical model of aluminium melting process was developed. It took into account coupling of electromagnetic and thermofluid fields that was performed using commercial codes. In the next step, the sensitivity analysis of turbulence modelling in the liquid domain was performed. The obtained numerical results were compared with the measurement data. The performed analysis can be treated as a preliminary approach for more complex mathematical modelling for the melting process optimisation in crucible induction furnaces of different types.

Keywords: induction furnace, crucible, coupled model, CFD, electromagnetism

W tej pracy przeprowadzono analizę pola prędkości i tworzących się wirów w tyglu typowego pieca indukcyjnego. W pierwszym etapie pracy zostały przeprowadzone pomiary kształtu powierzchni swobodnej ciekłego metalu na stanowisku z tyglem ceramicznym. Następnie został stworzony model numeryczny badanego tygla opisujący proces topienia aluminium. Model uwzględniał sprzężenie pola elektromagnetycznego oraz cieplno-przepływowego, które przeprowadzono za pomocą komercyjnych programów. Następnie przeprowadzono analizę wrażliwości ze względu na sposób modelowania turbulencji w ciekłym metalu. Wyniki numeryczne zostały porównane z danymi z eksperymentu. Przeprowadzona analiza pozwoli na stworzenie dokładniejszych modeli numerycznych umożliwiających odtworzenie pola prędkości ciekłego metalu i optymalizację procesu topienia w piecach indukcyjnych.

1. Introduction

The technology of metal melting in the induction furnace allows for efficient removal of impurities, thereby yielding products of very high purity. Then such materials can be applied in cutting edge technologies as aviation (turbine blades), biotechnology (prosthesis, implants), to name but a few. To control these processes, measurements and numerical analysis can be conducted. In this paper, the results of both experimental and numerical approaches were presented.

Review of literature shows clearly that the experimental portion of the research is by far more advanced than its modelling counterpart. Numerical models have to deal with coupling of electromagnetic and thermofluid phenomena [1-5]. Commonly, the computational domain was, as a rule, axisymmetric [6] though in the study [7], a 3-D segment with appropriately defined periodicity conditions [7] was considered. The metal flow in the crucible of induction furnace is turbulent. This means that the turbulence models need to be employed in the CFD modelling of such a process. The published information in the field are not consistent in terms of the use of a particular model. The most commonly used ones are based on the RANS formulation. The paper [8] gives the analysis of the influence of the turbulence intensity in the near surface zone of the metal onto the evaporation of components of the melt. However, the paper studies only classic turbulence k-epsilon and its RND variant [9], while the current trend is to use more sophisticated techniques, able to reproduce the behaviour of the fluid in the near-surface domains. Large Eddy Simulations (LES) [10] and Reynolds Stress Model are good examples of such approaches.

The aim of this work was to numerically investigate the velocity and turbulence fields inside the crucible of the induction furnace leading to the free surface shape prediction. For this reason, a numerical model of the coupled

* SILESIAN UNIVERSITY OF TECHNOLOGY, FACULTY OF ENERGY AND ENVIRONMENTAL ENGINEERING, INSTITUTE OF THERMAL TECHNOLOGY, 22 KONARSKIEGO STR., 44-100 GLIWICE, POLAND

** SILESIAN UNIVERSITY OF TECHNOLOGY, FACULTY OF MATERIALS ENGINEERING AND METALLURGY, DEPARTMENT OF INDUSTRIAL INFORMATICS, 8 KRASINSKIEGO STR., 40-019 KATOWICE, POLAND

*** SILESIAN UNIVERSITY OF TECHNOLOGY, FACULTY OF MATERIALS ENGINEERING AND METALLURGY, INSTITUTE OF METAL TECHNOLOGY, 8 KRASINSKIEGO STR., 40-019 KATOWICE, POLAND

Corresponding author: piotr.bulinski@polsl.pl

electromagnetic and thermal phenomena was developed. Then, an influence of different turbulence models was examined. Because of the low computing times, the three most popular RANS models were tested in this work.

2. Experiment

Due to high temperatures and proximity of the crucible, carrying out measurements in liquid metal is not a trivial matter. Thus, the measurements are conducted using contactless methods. In order to validate of the numerical model, the measurement test rig was constructed as shown in Figure 1. The inductor was placed on the movable table, therefore it was possible to estimate the effects of its position on the liquid/solid metal behaviour in the crucible. Several tests were carried out for different crucibles, currents, inductor positions, etc.

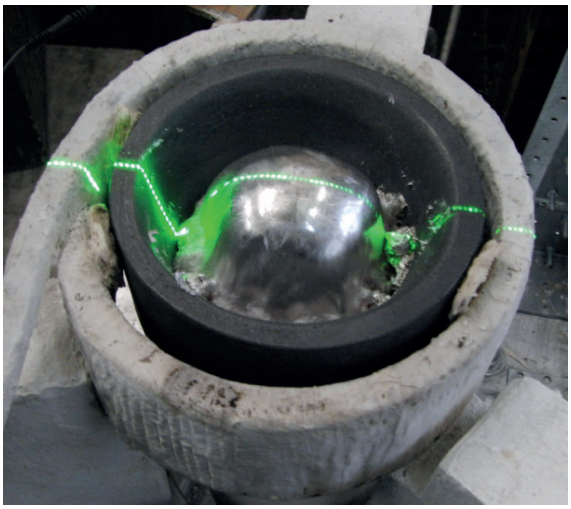

Fig. 1. Measurement test rig

The shape of liquid metal can be measured with radar sensors, ultrasonic and more frequently used laser sensors. In this study, it was necessary to scan the complete profile of the liquid metal surface with sufficient resolution. For this reason, the 3-D laser scan method [11] was adapted.

The laser measurement of the profile is carried out most frequently by triangulation method because of its precision and the relative simplicity [12, 13]. This technique is based on the projection of the laser beam on the surface and then registering the reflection beam by a camera. The scheme of measurement method was presented in Figure 2. A final shape of the surface of the crystallised liquid metal can be calculated using the following mathematical equations:

$$\begin{cases} y = \dfrac{c(b-x)}{L} - a \\ y = \tan(\beta)x \end{cases} \tag{1}$$

where: x, y are the coordinates of a point of the free surface of the liquid metal, β is a slope of the laser beam, L is a position of the laser spot on a camera sensor, a, b and c are the geometrical dimensions.

All the relations between the geometrical parameters are presented in Figure 2.

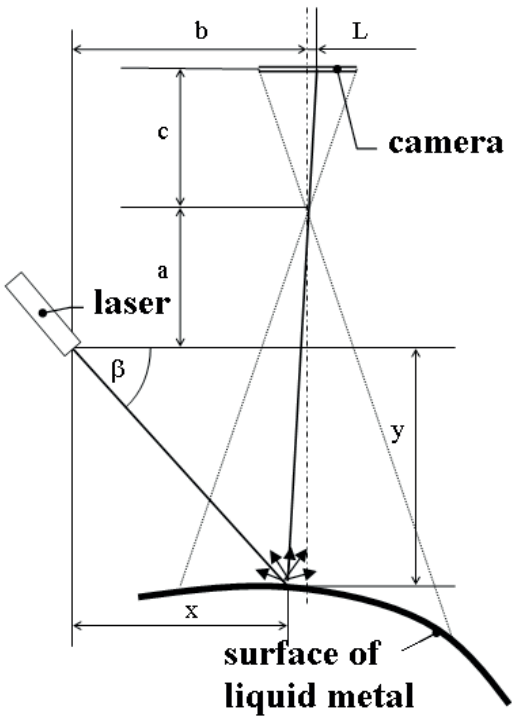

Fig. 2. Scheme of measurement method

3. Numerical model

The considered crucible is exposed to negligible both axial and tangential forces. Therefore, it was possible to simplify the model geometry to two-dimensional axisymmetric space. As shown in Figure 3, the numerical domain was bounded by of outlet, axis, side and bottom walls. The overall geometrical dimensions were the following: the outlet radius of 62 mm, the model height of 200 mm and a bottom radius of 30 mm. The molten metal sample had reached 128 mm height of the crucible.

For verification study, few cases with different grids were performed. This produced the most appropriate model setups for the final simulations. The employed numerical discretisation was shown in Figure 3(b). It contained 24 000 high quality quadrilaterals. According to the sensitivity analysis that was performed, this grid size was sufficient.

The coupled numerical model of the pure metal melting in the induction furnace was formulated using platforms of two commercial codes. Both component programs were mutually connected in an effective coupling procedure. Electromagnetic field was computed using Ansys Mechanical APDL 15. The solution was transferred to CFD solver, where a new shape of the liquid metal was determined. The new geometry was again solved using the electromagnetic solver and this loop was repeated during the whole simulation process. The calculations were performed in the transient mode. Two seconds of the real time were computed with the time steps of 0.0001 s. After every 100 time steps, the electromagnetic and flow fields were updated.

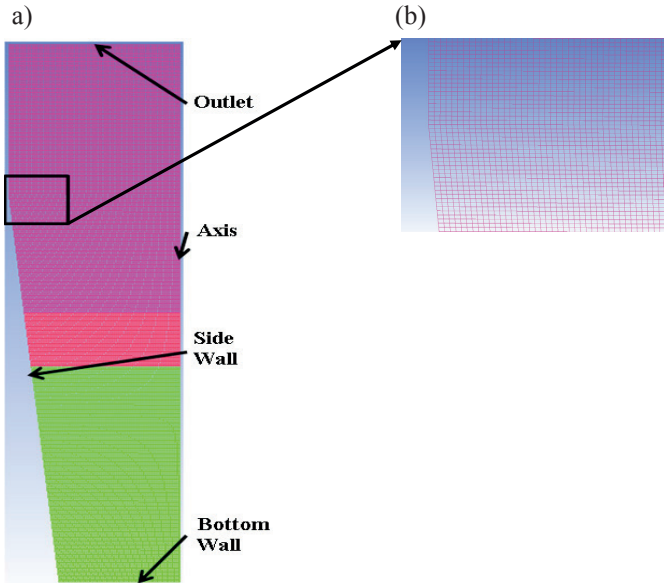

Fig. 3. (a) Boundary conditions and (b) a part of the numerical grid in the developed model

The formulated two-dimensional, axially symmetric electromagnetic model was based on a commonly used equation where the magnetic vector potential is applied:

$$\nabla\times\left(\frac{1}{\mu}\nabla\times\boldsymbol{A}\right)+\mathrm{j}\omega\sigma\boldsymbol{A}=\boldsymbol{J}_s \tag{2}$$

where: μ, σ is the magnetic permeability and conductivity of aluminium, ω is the angular frequency and J_s is the current density source.

On the basis of the distribution of the magnetic vector potential A, a distribution of the magnetic induction (Eq. 2), the eddy current densities (Eq. 3) and the density of electromagnetic force that acts on a liquid metal (Eq. 4) can be determined:

$$\boldsymbol{B}=\nabla\times\boldsymbol{A} \tag{3}$$

$$\mathbf{J}=-\mathrm{j}\omega\sigma\mathbf{A} \tag{4}$$

$$\boldsymbol{f}_e=\frac{1}{2}\mathrm{Re}\left(\boldsymbol{J}\times\boldsymbol{B}^*\right) \tag{5}$$

To predict a shape of free surface, it was necessary to solve the momentum conservation equations. For 2-D axisymmetric and unsteady flow, these equations take the following form:

$$\frac{\partial}{\partial t}(\rho v_x)+\frac{1}{r}\frac{\partial}{\partial x}(r\rho v_x v_x)+\frac{1}{r}\frac{\partial}{\partial r}(r\rho v_r v_x)=-\frac{\partial p}{\partial x}+\frac{1}{r}\frac{\partial}{\partial x}\left[r\mu\left(2\frac{\partial v_x}{\partial x}-\frac{2}{3}(\nabla\cdot\vec{v})\right)\right] \tag{6}$$
$$+\frac{1}{r}\frac{\partial}{\partial r}\left[r\mu\left(\frac{\partial v_x}{\partial r}+\frac{\partial v_r}{\partial x}\right)\right]+\rho\vec{g}+F_x$$

$$\frac{\partial}{\partial t}(\rho v_r)+\frac{1}{r}\frac{\partial}{\partial x}(r\rho v_x v_r)+\frac{1}{r}\frac{\partial}{\partial r}(r\rho v_r v_r)=-\frac{\partial p}{\partial r}+\frac{1}{r}\frac{\partial}{\partial x}\left[r\mu\left(\frac{\partial v_r}{\partial x}+\frac{\partial v_x}{\partial r}\right)\right] \tag{7}$$
$$+\frac{1}{r}\frac{\partial}{\partial r}\left[r\mu\left(2\frac{\partial v_r}{\partial r}-\frac{2}{3}(\nabla\cdot\vec{v})\right)\right]-2\mu\frac{v_r}{r^2}+\frac{2}{3}\frac{\mu}{r}(\nabla\cdot\vec{v})+F_r$$

where ρ is the density, t is the time, x and r are the axial and radial coordinates, respectively, v is the velocity vector, g is the gravity vector, μ is the dynamic viscosity and F_r, F_x are the components of the Lorentz force vector

In this study, a multiphase flow was simulated using Volume of Fluid (VOF) model. Moreover, the explicit temporal marching scheme was used. To track the interface between air and liquid/solid metal, the mass conservation equation for the volume fraction was solved:

$$\frac{\alpha_q^{n+1}\rho_q^{n+1}-\alpha_q^n\rho_q^n}{\Delta t}V+\sum_f\left(\rho_q U_f^n\alpha_{q,f}^n\right)=0 \tag{8}$$

where αq is the volume fraction of the current (n+1) and the previous (n) time step and U is the volume flux.

To solve the defined set of the differential equations, material properties of air and metal had to be specified. The liquid metal parameters were the density of 2380 kg/m^3 and the dynamic viscosity of 0.0015 kg/(m·s) which are the average values for the liquid aluminium at the temperature of 1500ºC. To simplify model, the air was defined as incompressible gas with the density of 1.225 kg/m^3 and the dynamic viscosity of 1.7894e-5 kg/(m·s).

4. Results

The simulations were performed in unsteady state to monitor the shape of free surface. In the Figure 4, the volume fraction of aluminum for six different time instants was presented. Figure 4(a) presents the initial state of the metal. It is a flat surface without any meniscus. Then after 0.01 s due to the surface tension and the contact angle between liquid aluminium and air, the natural meniscus is being formed. Once the Lorentz force from electromagnetic field starts acting, the surface of the liquid metal gradually rises. It achieved the maximum height after 0.17 s. At that moment, the meniscus started falling and finally reaching the minimum position. It happened after 0.37 s of the real time. After few oscillations, the metal surface has stabilised after 0.64 s reaching the quasi-steady state.

The final shape of the free surface for three different turbulence models were compared with measurement data. In Figure 5, the numerical solution was denoted with red points, while the measurement data are presented as blue points. For the considered turbulence models, CFD results are very accurate in the radius range of 0.02 m to 0.04 m from the crucible axis.

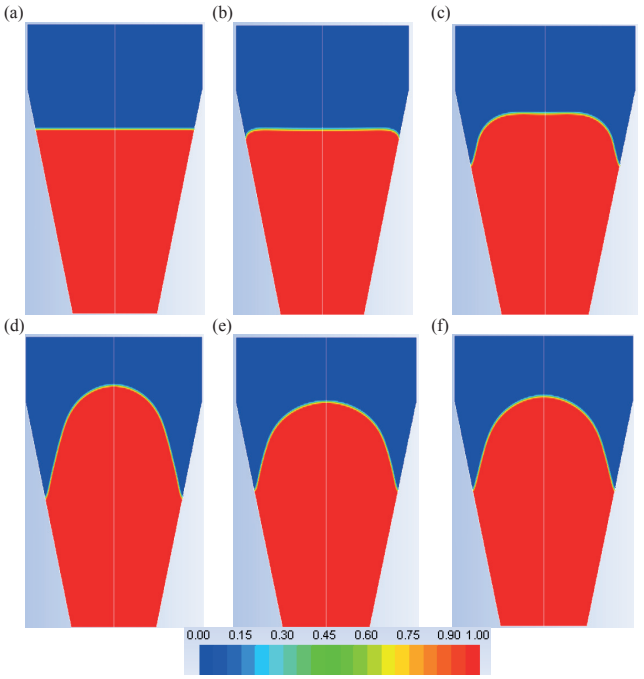

Fig. 4. The volume fraction of aluminium in the numerical domain for different time inants: (a) 0.00 s, (b) 0.01 s, (c) 0.05 s, (d) 0.17 s, (e) 0.37 s and (f) 0.64 s

The measurements were performed without atmosphere of inert gases, Therefore, the products of the oxidation accumulated near the crucible wall. This resulted in the flat meniscus near wall. In the numerical model, the oxides did not appear because the chemical reactions were not taken into account. There is also a difference between the measurements and the numerical simulations in the axis region. The metal melting process is very unsteady and, as a consequence, the free surface is oscillating up and down. However, the camera did not perform the time averaging. Hence, the results showed the field for a given time instant. The most accurate turbulence model was the RNG k-ε formulation, while for other models, the meniscus was slightly higher. For all the turbulence models, the contact of the liquid metal and the crucible wall was at the same height.

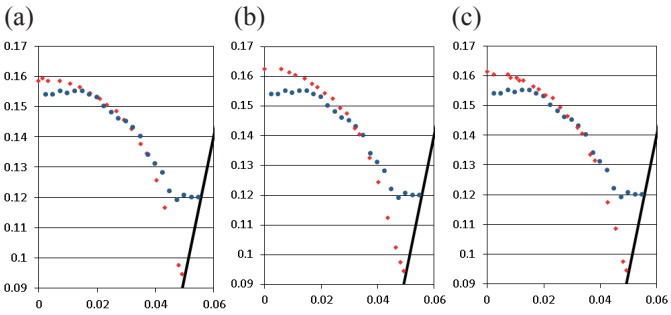

Fig. 5. Profile of the liquid metal surface for CFD solution (red points) and measurement results (blue points) inside a crucible space (in mm) for different turbulence models: (a) *k-ε*, (b) *k-ω* and (c) transition SST

The main impact on the shape of free surface had the Lorentz force. There was no difference in its distribution for different turbulence models. A typical vector distribution of the Lorentz force were presented in Figure 6 for the RNG *k-ε* turbulence model. The highest force acted near the contact point of the liquid metal and the crucible wall. Its value was approximately 500 kN and it was similar for all the considered turbulence models. It can also be observed that the Lorentz force affects only the outer areas of the liquid metal.

A distribution of the Lorentz force in the numerical domain entailed the velocity field inside the liquid metal as presented in Figure 7. However, the velocity vectors for every turbulence model are similar. There are two large eddies at the bottom of the liquid metal and two smaller on the top. The stagnation area appeared on the same height as the contact spot of the metal and crucible wall. It is associated with the highest values of the Lorentz force in this region.

A comparison of the velocity fields obtained for different turbulence models shows that the highest velocities were observed for the transition SST model. The lowest values of velocities were characteristic for the RNG k-ε approach. This can be attributed by the higher turbulence viscosity of this model. Moreover, it also had an influence on the free surface shape because the liquid metal reached higher position for standard k-ω and transition SST models than in the case of the RNG k-ε model. The differences in the velocity values on the liquid metal surface were noticed as well. This observation is to be examined in the future experiments in which the surface velocity will be measured.

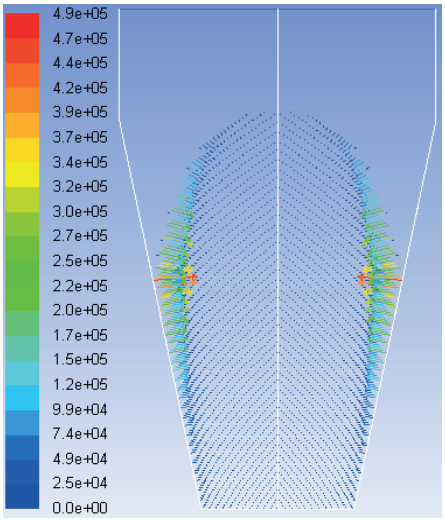

Fig. 6. The Lorentz force vector (in N) for the RNG k-ε test case

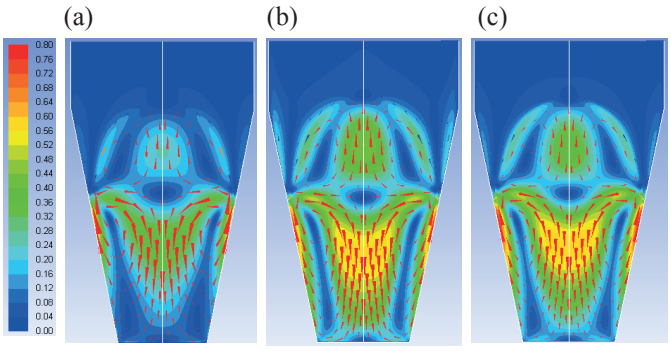

Fig. 7. The velocity vector fields (in m/s) for different turbulence models: (a) *k-ε*, (b) *k-ω*, and (c) transition SST

5. Summary

In this work, the influence of the RANS turbulence models on the free surface shape and the velocity field in the typical crucible induction furnace was analysed. The numerical solutions was compared with the experimental data obtained for the aluminium melting process. The validation of the numerical models showed that RANS models gave similar results for the free surface profile. However, the most accurate turbulence model turned out to be the RNG k-ε formulation. For that model, the velocity values inside the crucible were the smallest. The highest velocities were obtained for the transition SST model. There was no significant difference in the Lorentz force distribution for different turbulence modelling methods.

Acknowledgements

Financial assistance was provided by grant no. 2014/13/B/ST8/02364 funded by the National Science Centre, Poland, and is here acknowledged.

REFERENCES

[1] V. Bojarevics, R.A. Harding, M. Wickins, Experimental and numerical study of the cold crucible melting process, Proceeding of the Third International Conference on CFD in the Minerals and Process Industries, CSIRO (2003).

[2] J.H. Songa, B.T. Mina, An electromagnetic and thermal analysis of a cold crucible melting, International Communications in Heat and Mass Transfer 32, 1325-1336 (2005).

[3] S. Spitans, A. Jakovics, E. Baake, B. Nacke, Numerical modelling of free surface dynamics of conductive melt in the induction crucible furnace, Magnetohydrodynamics **46**, 317-328 (2010).

[4] S. Spitans, A. Jakovics, E. Baake, B. Nacke, Numerical modelling of free surface dynamics of melt in an alternate electromagnetic field, Magnetohydrodynamics **4**, 461-473 (2011).

[5] S. Spitans, A. Jakovics, E. Baake, B. Nacke, Numerical modelling of free surface dynamics of melt in alternate electromagnetic field, Journal of Iron and Steel Research, International **19**, 531-535 (2012).

[6] J. Yang, R. Chen, H. Ding, J. Guo, J. Han, H. Fu, Thermal characteristics of induction heating in cold crucible used for directional solidification, Applied Thermal Engineering **59**, 69-76 (2013).

[7] I. Quintana, Z. Azpilgain, D. Pardo, I. Hurtado, Numerical modeling of cold crucible induction melting, Proceedings of The COMSOL Conference, Boston, USA (2011).

[8] K. Adler, R. Schwarze, V Galindo, Numerical modelling of the evaporation process of an electromagnetically stirred copper melt, Proceedings of the FLUENT CFD Forum 2005, Bad Nauheim, Germany (2005).

[9] T. Toh, H. Yamamura, H. Kondo, M. Wakoh, S. Shimasak, S. Taniguchi, Kinetics evaluation of inclusions removal during levitation melting of steel in cold crucible, ISIJ International **47**, 1625-1632 (2007).

[10] A. Umbrasko, E. Baake, B. Nacke, A. Jakovics, Numerical studies of the melting process in the induction furnace with cold crucible, COMPEL: The International Journal for Computation and Mathematics in Electrical and Electronic Engineering **27**, 359-368 (2008).

[11] S. Golak, Application of image analysis for the measurement of liquid metal surface, Transactions on Modelling and Simulation, WIT 48 (2009).

[12] H.G. Mass, B. Hentschel, F. Schreiber, An optical triangulation method for height measurements on water surfaces, SPIE Proceedings Series 5013, 103-109 (2003).

[13] C. Mulsow, M. Schulze, P. Westfeld, An optical triangulation method for height measurements on instationary water surfaces, IAPRS Volume XXXVI 5 (2006).

Received: 20 September 2014.